Original Article

HSPB1 silencing enhances ferroptosis in glioma cells by suppressing BAG3 expression

Qin Li¹, Honggang Ma¹, Zi Ye², Leiming Huo¹

¹Department of Surgery II, Shenzhen Bao'an Hospital of Traditional Chinese Medicine, Shenzhen 518100, Guangdong, China; ²Department of Traditional Chinese Medicine, The Second People's Hospital of Guangdong Province, Guangzhou 510317, Guangdong, China

Received June 18, 2025; Accepted August 29, 2025; Epub September 15, 2025; Published September 30, 2025

Abstract: Objectives: To investigate the role of heat shock protein family B (small) member 1 (HSPB1) in regulating ferroptosis in glioma and to explore the underlying molecular mechanisms. Methods: HSPB1 expression was analyzed in glioma cell lines. U251 glioma cells were transfected with HSPB1-targeting short hairpin RNA (shRNA). Cell proliferation, invasion, ferroptosis markers (iron accumulation, oxidative stress), and expression of BCL2-associated athanogene 3 (BAG3) were assessed using molecular and biochemical assays. BAG3 was further silenced or over-expressed to evaluate its interaction with HSPB1 in regulating ferroptosis. Results: HSPB1 was markedly overexpressed in glioma cell lines. HSPB1 knockdown significantly suppressed U251 cell proliferation and invasion, while promoting ferroptosis via increased intracellular Fe²⁺ levels and lipid peroxidation. BAG3 was identified as a downstream target of HSPB1. Silencing BAG3 replicated the anti-tumor and pro-ferroptotic effects of HSPB1 knockdown. Moreover, BAG3 overexpression partially rescued the effects of HSPB1 silencing, confirming its role in the HSPB1-mediated ferroptosis pathway. Conclusions: HSPB1 inhibits ferroptosis and promotes glioma cell survival, at least in part through BAG3 upregulation. Targeting the HSPB1-BAG3 axis may represent a novel therapeutic strategy and prognostic approach in glioma treatment.

Keywords: Glioma, ferroptosis, HSPB1, BAG3

Introduction

Gliomas are the most common type of primary malignant tumor in the central nervous system (CNS), originating from neuroepithelial cells and accounting for approximately 81.0% of all primary CNS malignancies. In China, the annual incidence of glioma is estimated at 8-10 per 100,000 individuals, with a five-year mortality rate second only to pancreatic and lung cancers among all systemic malignancies [1, 2]. Due to their highly infiltrative growth pattern and poorly defined tumor margins, complete surgical resection is often unachievable, resulting in high postoperative recurrence rates and poor clinical outcomes. Although current treatment regimens - including surgery, radiotherapy, chemotherapy, and their combinations offer some therapeutic benefits, overall efficacy remains limited. Moreover, the absence of reliable biomarkers for early diagnosis and prognosis continues to pose a major challenge in glioma management. Thus, a deeper understanding of the molecular mechanisms underlying glioma development and progression is urgently needed to support the design of more effective treatment strategies.

Ferroptosis is a recently characterized, irondependent form of regulated cell death, marked by excessive iron accumulation and lipid peroxidation. Glutathione peroxidase 4 (GPX4) plays a key role in protecting cells against ferroptosis by neutralizing lipid peroxides. Ferroptosis inducers such as erastin trigger cell death by directly or indirectly inhibiting GPX4, reducing antioxidant defenses, and promoting the accumulation of reactive oxygen species (ROS), ultimately leading to oxidative damage and cell death [3]. Morphologically, ferroptotic cells exhibit distinct mitochondrial changes, including reduced size and increased membrane density. In addition to GPX4, ferroptosis is accompanied by altered expression of several key genes such as acyl-CoA synthetase long-chain family member 4 (ACSL4) and transferrin receptor protein 1 (TFR1) [4].

Growing evidence suggests that ferroptosis plays a critical role in tumor progression and response to therapy. For instance, erastin has been shown to enhance the efficacy of chemotherapeutic agents such as cisplatin, doxorubicin, cytarabine, and temozolomide [5, 6]. In ovarian cancer, obacunone induces ferroptosis via a ROS-dependent mechanism, thereby improving treatment outcomes [7]. Similarly, in non-small cell lung cancer, erastin enhances docetaxel sensitivity by depleting glutathione (GSH) and inactivating GSH peroxidases [8]. In glioma, ferroptosis induction has also demonstrated therapeutic potential. Inhibition or knockout of GPX4 leads to the accumulation of lipid peroxides, causing membrane damage and cell death [9-11]. Paeoniflorin acetate, for example, exerts anti-tumor effects in glioma by suppressing the GPX4 pathway and triggering ferroptosis [12]. These findings collectively underscore the potential of targeting ferroptosis as an anticancer strategy.

Heat shock protein family B (small) member 1 (HSPB1), also known as Hsp27, is a cytoplasmic heat shock protein involved in maintaining cellular homeostasis under stress conditions. It exhibits antioxidant, anti-apoptotic, and antiinflammatory functions. Under stress, HSPB1 expression is markedly upregulated, and the protein translocates into the nucleus, where it acts as a molecular chaperone to assist protein folding. Aberrant overexpression of HSPB1 has been reported in various tumor types [13, 14]. In glioma, elevated HSPB1 expression is strongly associated with tumor progression and poor prognosis, promoting cell proliferation and invasiveness [15, 16]. Consequently, HSPB1 has been proposed as a potential biomarker for glioma malignancy and outcome prediction.

Recent studies have identified HSPB1 as a negative regulator of ferroptosis. Downregulation of HSPB1 enhances erastin-induced ferroptosis in cancer cells [17]. Meng et al. reported that erastin upregulates HSPB1 expression, while HSPB1 knockdown significantly increases erastin-induced cell death [18]. In addition, inhibition of protein kinase C prevents HSPB1 phosphorylation, thereby promoting iron uptake

and lipid peroxidation and enhancing ferroptosis.

Based on this background, we hypothesize that HSPB1 regulates ferroptosis in glioma cells and consequently modulates malignant tumor behavior. Furthermore, we aim to elucidate the molecular mechanisms through which HSPB1 participates in ferroptosis regulation. These findings may offer new insights into glioma pathogenesis and support the development of ferroptosis-targeted therapeutic strategies.

Materials and methods

Cells and transfection

The human glioma cell lines U138MG, A172. and U251, along with the immortalized human astrocyte cell line SVG p12, were obtained from the American Type Culture Collection. Cells were cultured in DMEM (Gibco, Rockville, MD) supplemented with 10% fetal bovine serum (FBS) and 1% penicillin-streptomycin at 37°C in a humidified incubator containing 5% CO_a. Plasmids for BCL2-associated athanogene 3 overexpression (BAG3-OE) and corresponding empty vectors were purchased from RiboBio Co., Ltd. (Guangzhou, China). Short hairpin RNAs targeting HSPB1 (HSPB1-shRNA) and BAG3 (BAG3-shRNA), along with their respective non-targeting controls (Mock), were obtained from Santa Cruz Biotechnology (Santa Cruz, CA, USA). Transfections were performed using the appropriate reagents according to the manufacturers' protocols.

RT-qPCR

Total RNA was extracted from cells using TRIzol reagent (Invitrogen, MA, USA), following the manufacturer's instructions. Complementary DNA was synthesized using the PrimeScript RT Kit (Takara, China). qRT-PCR was performed using specific primers for HSPB1, BAG3, and GAPDH (internal control). All primers were synthesized by Sangon Biotech (Shanghai, China), with the following sequences:

(1) HSPB1: forward 5'-CGT ATG GTT CAG TCG TCA TTG-3', reverse 5'-GCG GAG TAC GTC CGC GTA G-3'. (2) BAG3: forward 5'-CCA TGA CCC ATC GAG AAA CTG C-3', reverse 5'-GCT GGG AGG ACA AGG AAC TG-3'. (3) GAPDH: forward 5'-CGG AGT CAA CGG ATT TGG TCG TAT-3',

reverse 5'-AGC CTT CTC CAT GGT GGT GAA GAC-3'.

Relative mRNA expression was calculated using the 2^- $\Delta\Delta$ Ct method and normalized to GAPDH.

Western blotting

Total protein was isolated from cultured cells using RIPA lysis buffer. After quantification, equal amounts of protein were separated by SDS-PAGE and transferred to polyvinylidene fluoride membranes (Bio-Rad, CA, USA). Membranes were blocked with 5% non-fat milk in Tris-buffered saline containing Tween-20 for 2 hours at room temperature, followed by overnight incubation at 4°C with the following primary antibodies (Abcam, UK):

GAPDH (1:5000), HSPB1 (1:3000), BAG3 (1:5000), GPX4 (1:4000), and TFR1 (1:1000).

After washing, membranes were incubated with HRP-conjugated secondary antibodies for 2 hours at room temperature. Protein bands were visualized using an enhanced chemiluminescence system and quantified using ImageJ software.

Transwell invasion assay

U251 cells were serum-starved for 12 hours in RPMI-1640 medium without FBS. Cells were then washed with PBS, resuspended, and counted. A total of 200 μL of the cell suspension was seeded into the upper chamber of Matrigel-coated Transwell inserts (BD Biosciences, USA), while 700 μL of RPMI-1640 medium containing 10% FBS was added to the lower chamber as a chemoattractant. The plates were incubated at 37°C with 5% CO $_2$ for 48 hours.

After incubation, non-invading cells on the upper surface of the membrane were removed with a cotton swab. Cells that had migrated to the lower surface were fixed with formaldehyde for 10 minutes, air-dried, and stained with 0.1% crystal violet for 20 minutes. After rinsing with PBS and drying, five random fields were selected under a light microscope for imaging and cell counting.

Plate clonogenic assay

U251 cells were seeded in 6-well plates and cultured under standard conditions for 14 days.

On day 15, the culture medium was discarded and the wells were gently washed with PBS. Cells were fixed with 1 mL of 4% paraformaldehyde for 15 minutes at room temperature, followed by staining with 1 mL of crystal violet for 2 minutes. Excess stain was removed by repeated PBS washing. Colonies containing more than 50 cells were counted under a light microscope, and colony formation efficiency was analyzed.

GSH quantification

Cells were harvested by trypsinization using 0.25% trypsin for 5 minutes and centrifuged at 5,000×g for 10 minutes. The cell pellet was resuspended in PBS and subjected to sonication for lysis. After a second centrifugation at 5,000×g for 10 minutes, the supernatant was collected. Intracellular GSH levels were measured using a commercial assay kit, following the manufacturer's instructions, based on sample absorbance readings.

ROS measurements

Intracellular reactive oxygen species (ROS) were measured using 2',7'-dichlorodihydrofluorescein diacetate (DCFH-DA). Cells were incubated with 10 μ M DCFH-DA at 37°C for 20 minutes. After incubation, cells were trypsinized, resuspended in PBS, and centrifuged at 1,000×g for 10 minutes. The pellet was washed three times with PBS to remove residual dye. Fluorescence intensity, indicating ROS production, was detected using either a fluorescence microscope or an immunofluorescence microplate reader. Oxidation of DCFH-DA to fluorescent DCF served as an indicator of ROS generation.

MDA assay

Malondialdehyde (MDA) levels were assessed using a commercial assay kit following the manufacturer's instructions. Briefly, 100 μL of absolute ethanol (blank), standard solution, or sample lysate was mixed with 1 mL of freshly prepared working reagent. Samples were incubated in a boiling water bath (100°C) for 40 minutes, cooled to room temperature, and centrifuged at 1,000×g for 10 minutes. The supernatant was transferred to a 96-well plate and incubated in the dark for 60 minutes. Absorbance was measured at 532 nm using a

microplate reader, and MDA concentrations were calculated based on the standard curve.

Lipid peroxidation assay

Lipid peroxidation was assessed using the fluorescent probe C11-BODIPY 581/591. Following treatment, cells were harvested with 0.25% trypsin for 10 minutes, and the reaction was stopped with complete medium. After centrifugation at 1,000×g for 5 minutes, the cell pellet was resuspended in pre-warmed buffer containing 10 μ M C11-BODIPY 581/591 and incubated at 37°C in the dark for 1 hour. Cells were then centrifuged again, washed, and resuspended in fresh buffer. Fluorescence was detected using a flow cytometer with a 488 nm excitation laser, and data were analyzed using FlowJo software.

CO-IP assay

Cells were washed twice with ice-cold PBS and lysed in pre-chilled lysis buffer. Lysates were incubated on ice for 10 minutes and sonicated for complete disruption. After centrifugation at 13,000×g for 10 minutes at 4°C, the supernatant was collected. FLAG magnetic beads were prewashed with PBS and incubated with the lysates overnight at 4°C with gentle rotation. After incubation, the beads were washed twice with lysis buffer, vortexed, and centrifuged at 5,000×g for 5 minutes. The final pellet was resuspended in 35 μL of lysis buffer with 10 μL of 6× SDS loading buffer and boiled at 100°C for 10 minutes. Eluted proteins were analyzed by Western blotting.

Intracellular Fe²⁺ quantification

Cells were trypsinized and resuspended in fresh DMEM with 10% FBS. After counting, equal numbers of cells were collected and washed twice with ice-cold PBS. The cell pellet was resuspended in lysis buffer, sonicated on ice for 5 minutes, and incubated for an additional 2 hours. Samples were centrifuged at 13,000×g for 10 minutes at 4°C. Supernatants were collected, and intracellular Fe²⁺ concentrations were determined using a commercial ferrous ion detection kit (Cat. No. E1042), following the manufacturer's protocol.

Lactate dehydrogenase (LDH) release assay

U251 cells were seeded into 96-well plates and allowed to adhere overnight. According to the

experimental groups, the culture supernatant was collected and mixed with the LDH reaction mixture. After 30 minutes of incubation at room temperature in the dark, absorbance was measured at 490 nm. The percentage of LDH release was calculated according to the manufacturer's formula.

CCK-8 assay

U251 cells were seeded into 96-well plates and cultured overnight. According to experimental groupings, 10 μ L of CCK-8 solution was added to each well. Plates were incubated at 37°C for 2 hours, and absorbance was measured at 450 nm. Cell viability was calculated as a percentage relative to the control group.

Statistical analysis

All data were analyzed using SPSS 22.0 software. Quantitative data are presented as mean ± standard deviation (SD) from at least three independent experiments. Comparisons between the two groups were performed using the Student's t-test, while comparisons among multiple groups were analyzed by one-way analysis of variance (ANOVA). A *P*-value <0.05 was considered statistically significant.

Results

Knockdown of HSPB1 inhibits the malignant growth of U251 cells

Bioinformatics analysis revealed that HSPB1 is abnormally overexpressed in a variety of malignancies, including glioblastoma (**Figure 1A**). As shown in **Figure 1B**, HSPB1 expression was significantly higher in glioblastoma tissues (n=163) compared to normal brain tissues (n=207). Moreover, glioma patients with high HSPB1 expression exhibited significantly shorter overall survival than those with low expression levels (**Figure 1C**), suggesting a potential oncogenic role of HSPB1 in glioma development.

Consistently, HSPB1 protein expression was also upregulated in glioma cell lines compared to normal human astrocytes (Figure 1D). Among three different short hairpin RNAs targeting HSPB1, all effectively reduced both mRNA (Figure 1E) and protein (Figure 1F) levels, with HSPB1-sh1 demonstrating the highest silencing efficiency and thus selected for subsequent

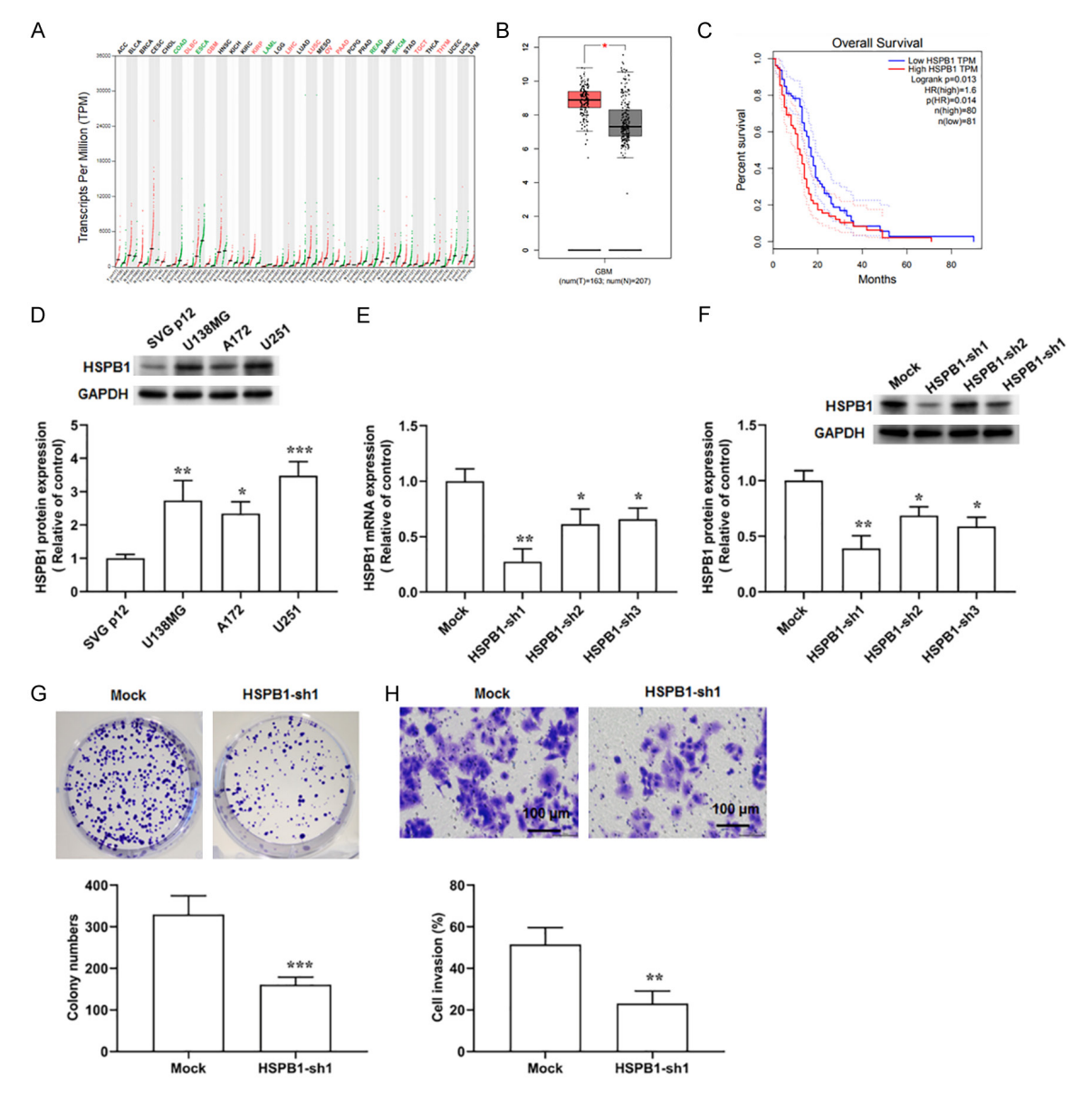


Figure 1. Expression level of HSPB1 in gliomas. A and B. Expression levels of heat shock protein family B (small) member 1 (HSPB1) in various malignant tumors and gliomas (http://gepia.cancer-pku.cn/). C. Association between HSPB1 expression and overall survival (http://gepia.cancer-pku.cn/). D. Protein expression levels of HSPB1 in tumor cell lines. E and F. Knockdown efficiency of HSPB1. G. Proliferation ability of U251 cells. H. Cell invasion. Scale bar =100 µm. N=5. *P<0.05. **P<0.01. ***P<0.001.

experiments. Functionally, HSPB1 knockdown significantly suppressed the proliferation (Figure 1G) and invasion (Figure 1H) of U251 cells, indicating that HSPB1 promotes glioma cell malignancy and may act as an oncogenic factor.

Knockdown of HSPB1 promotes ferroptosis in U251 cells

To explore whether HSPB1 regulates ferroptosis during glioma progression, U251 cells were

transfected with HSPB1-sh1 and examined for ferroptosis-related markers. Knockdown of HSPB1 led to a significant decrease in intracellular GSH levels (Figure 2A) and GPX activity (Figure 2B), along with increased levels of reactive oxygen species (ROS) (Figure 2C), Fe²⁺ (Figure 2D), and MDA (Figure 2E).

Western blot analysis revealed that HSPB1 silencing reduced GPX4 expression while upregulating transferrin receptor protein 1 (TFR1) expression (**Figure 2F**). Additionally, an increase

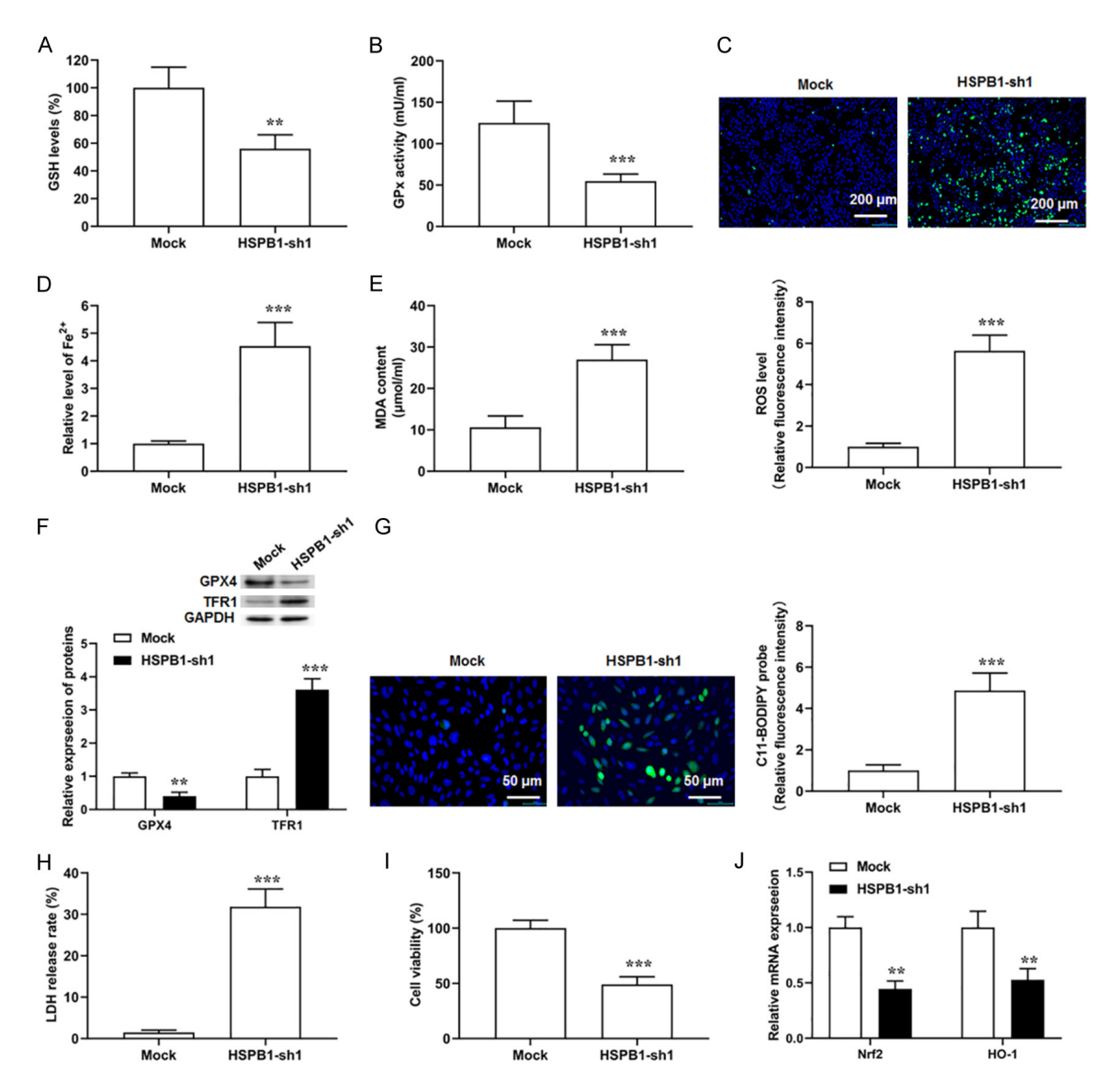


Figure 2. The effect of HSPB1 on ferroptosis in U251 cells. A. Glutathione (GSH) levels. B. GPx activity. C. Reactive oxygen species (ROS) levels detected by DCFH-DA fluorescence probe. Scale bar =200 μ m. D. Fe²⁺ accumulation levels. E. MDA content. F. Protein expression levels of glutathione peroxidase 4 (GPX4) and transferrin receptor protein 1 (TFR1). G. Lipid peroxidation levels indicated by BODIPYTM 581/591 C11 fluorescence probe. Scale bar =50 μ m. H. Lactate dehydrogenase (LDH) release rate assay. I. Cell viability. J. The mRNA expression of nuclear factor erythroid 2-related factor 2 (Nrf2) and heme oxygenase-1 (HO-1). N=5. **P<0.001.

in BODIPY™ 581/591 C11 fluorescence was observed in HSPB1-knockdown cells, indicating enhanced lipid peroxidation (Figure 2G). LDH release was significantly elevated (Figure 2H), and cell viability was decreased (Figure 2I), further supporting increased ferroptotic activity.

RT-qPCR analysis showed that knockdown of HSPB1 also suppressed the expression of Nrf2 and HO-1 (Figure 2J), components of the Nrf2/HO-1 antioxidant pathway, which is known to

protect cells from ferroptosis. Together, these findings indicate that HSPB1 downregulation promotes ferroptosis in U251 cells by modulating iron metabolism, oxidative stress, and suppressing antioxidant defenses.

Knockdown of HSPB1 suppresses BAG3 expression

Bioinformatics analysis and literature review identified BAG3, an anti-apoptotic protein fre-

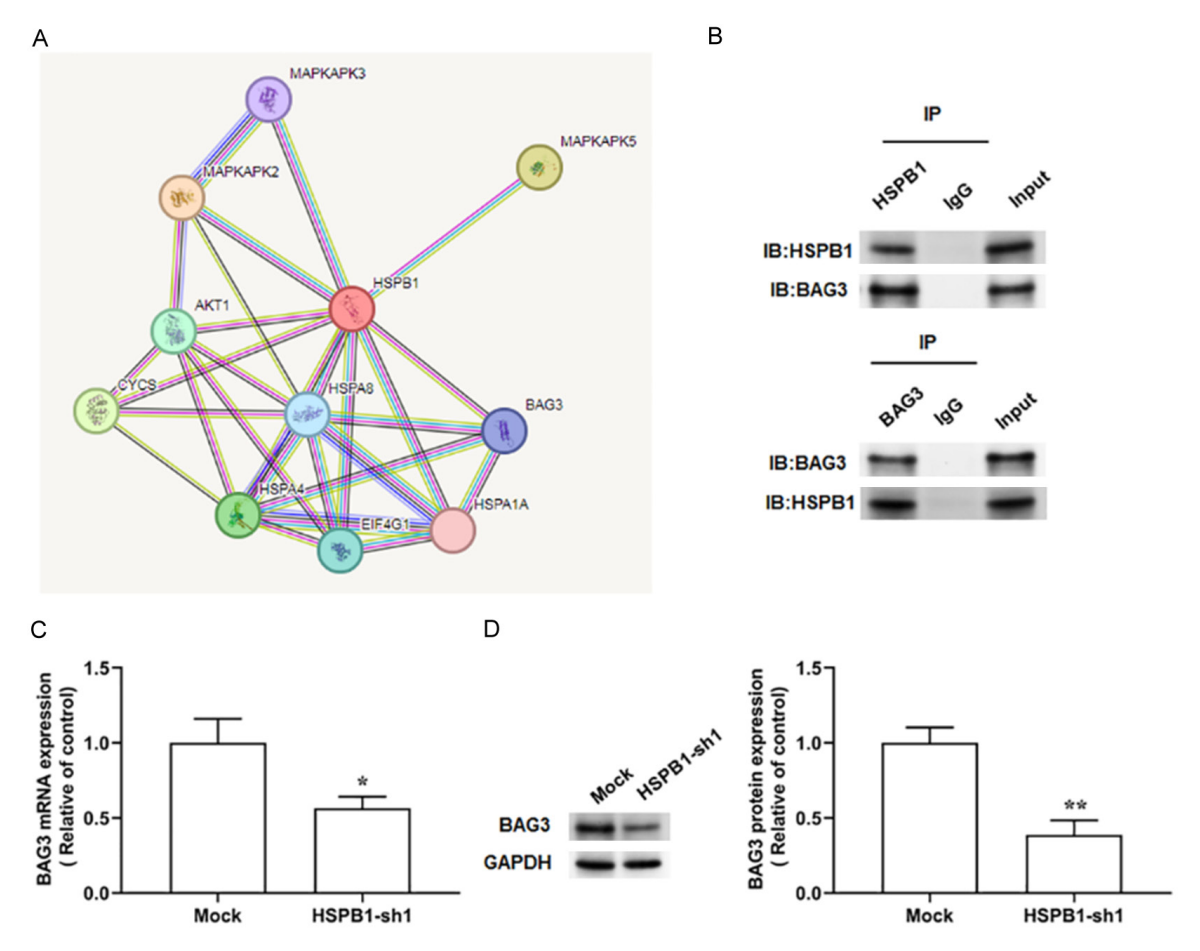


Figure 3. BCL2 associated athanogene 3 (BAG3) is a binding partner of HSPB1. A. Prediction of HSPB1-interacting proteins using online bioinformatics databases (https://cn.string-db.org/; https://thebiogrid.org/). B. Validation of the interaction between HSPB1 and BAG3 by Co-IP assay. C and D. Effect of HSPB1 knockdown on BAG3 mRNA and protein expression levels. N=5. *P<0.05. **P<0.01.

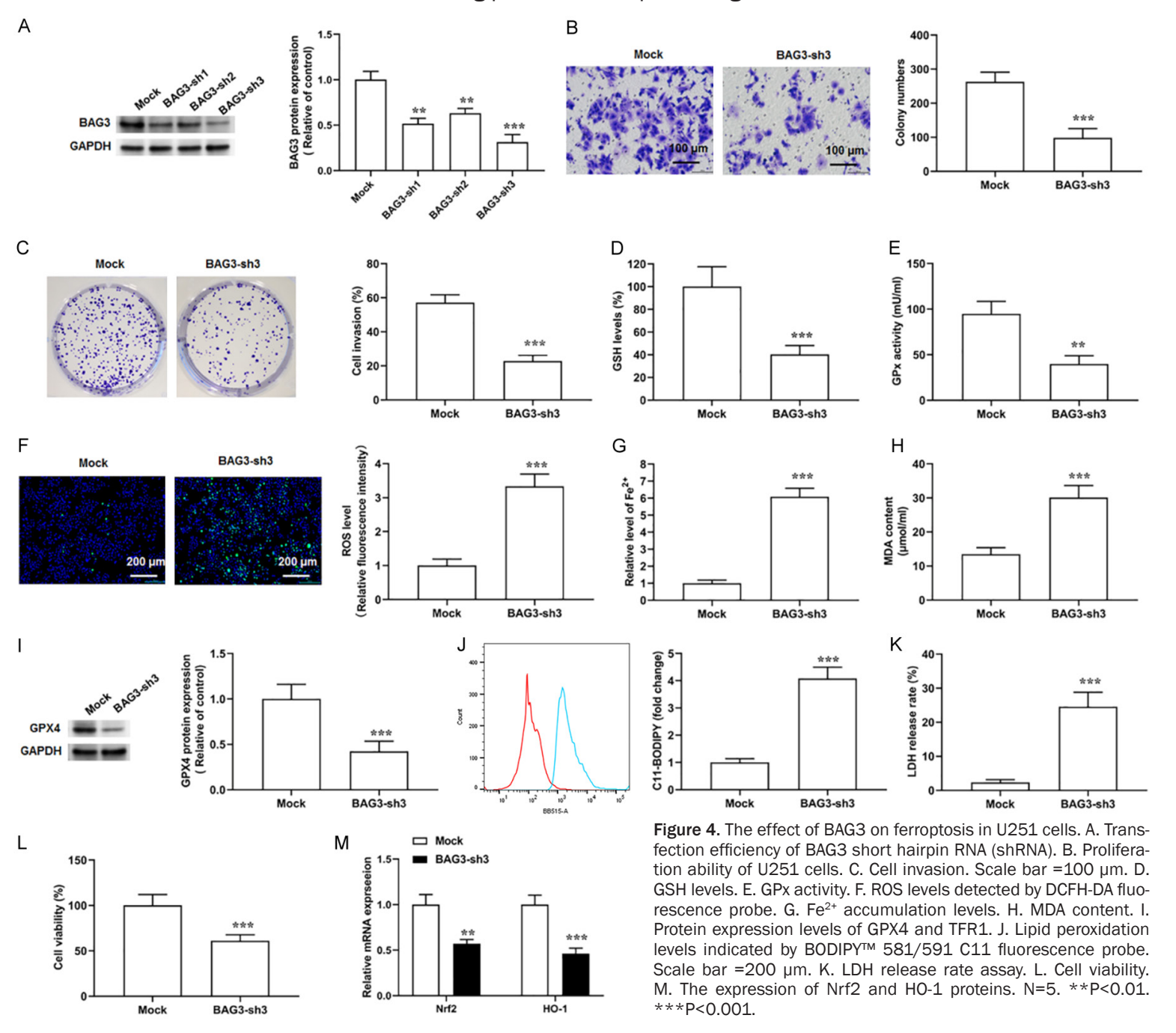
quently upregulated in cancer, as a potential binding partner of HSPB1 (Figure 3A). Co-IP assays confirmed a direct physical interaction between HSPB1 and BAG3 in U251 cells (Figure 3B). Subsequent transfection of HSPB1-sh1 into U251 cells significantly reduced both BAG3 mRNA (Figure 3C) and protein (Figure 3D) expression levels, as shown by RT-qPCR and Western blotting, respectively. These results suggest that HSPB1 positively regulates BAG3 expression in glioma cells.

Knockdown of BAG3 promotes ferroptosis in U251 cells

Three different short hairpin RNAs targeting BAG3 were transfected into U251 cells, and transfection efficiency is shown in **Figure 4A**. Among them, BAG3-sh3 exhibited the highest silencing efficiency and was selected for sub-

sequent experiments. Similar to HSPB1 knockdown, BAG3 silencing significantly suppressed U251 cell proliferation (**Figure 4B**) and invasion (**Figure 4C**).

Furthermore, BAG3 knockdown markedly reduced intracellular GSH levels (Figure 4D) and GPX activity (Figure 4E), while increasing ROS production (Figure 4F), Fe²⁺ accumulation (Figure 4G), and MDA content (Figure 4H). Western blot analysis confirmed that GPX4 protein expression was downregulated following BAG3 silencing (Figure 4I). Flow cytometry also revealed elevated lipid peroxidation in BAG3-knockdown cells (Figure 4J). Consistently, LDH release was enhanced (Figure 4K), cell viability was reduced (Figure 4L), and mRNA levels of Nrf2 and HO-1 were significantly suppressed (Figure 4M).



HSPB1 suppresses ferroptosis in U251 cells via BAG3

To investigate whether BAG3 mediates the antiferroptotic function of HSPB1, BAG3-sh3 was transfected alone or co-transfected with an HSPB1 overexpression plasmid (HSPB1-OE) into U251 cells. RT-qPCR confirmed increased HSPB1 mRNA expression following HSPB1-OE transfection (Figure 5A).

Western blot results showed that BAG3 knockdown reduced the protein expression of Nrf2 and H0-1, and this reduction was not reversed by HSPB1 overexpression. These findings suggest that in the absence of its binding partner BAG3, HSPB1 is unable to regulate the Nrf2/H0-1 pathway (**Figure 5B**). Treatment with erastin, a known ferroptosis inducer, further downregulated Nrf2 and H0-1 protein levels, producing effects comparable to those of BAG3 knockdown. Notably, BAG3 silencing in combination with erastin treatment produced a more pronounced ferroptotic response than erastin alone.

Functionally, BAG3 knockdown increased LDH release (**Figure 5C**), decreased cell viability (**Figure 5D**), and elevated intracellular Fe²⁺ (**Figure 5E**) and MDA (**Figure 5F**) levels. It also led to GSH depletion (**Figure 5G**) and reduced GPX4 expression (**Figure 5H**). Importantly, overexpression of HSPB1 failed to rescue these effects, indicating that BAG3 is essential for HSPB1-mediated suppression of ferroptosis.

Discussion

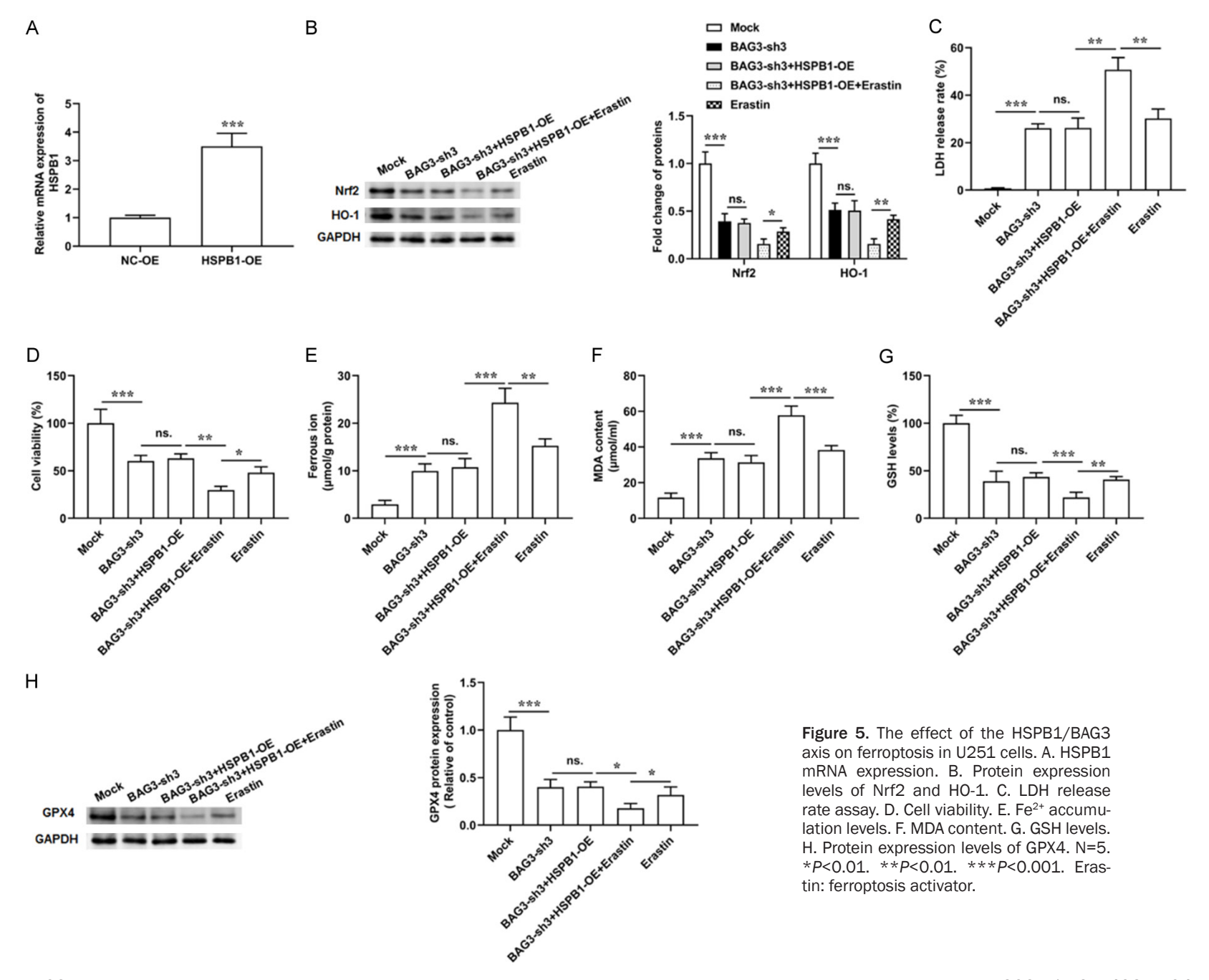
As the most common and aggressive type of neurological tumor, the incidence of gliomas continues to rise. The identification of gliomas specific biomarkers is expected to provide valuable therapeutic and prognostic insights, ultimately improving patient survival and quality of life. Ferroptosis is a distinct form of iron-dependent programmed cell death characterized primarily by the accumulation of lipid peroxides. In recent years, increasing attention has been directed toward ferroptosis in the context of cancer therapy, with the modulation of this process emerging as a promising strategy for treating malignancies, including gliomas.

HSPB1, a member of the small heat shock protein family, is a highly conserved protein that is

upregulated under various stress conditions. It has been implicated in the progression of multiple cancer types. High HSPB1 expression has been associated with metastasis and poor prognosis in breast cancer, where it can inhibit ferroptosis by activating the NF-kB signaling pathway, thus reducing the therapeutic efficacy of doxorubicin [19]. Similarly, in hepatocellular carcinoma, HSPB1 is significantly upregulated in tumor tissues and correlates with adverse clinical outcomes [20].

In our study, we found that HSPB1 expression was markedly elevated in glioma cell lines. Silencing HSPB1 significantly inhibited the proliferation and invasion of U251 glioma cells. HSPB1 has previously been identified as a negative regulator of ferroptosis. One study reported that HSPB1 knockdown in glioma cells promotes iron accumulation and ROS production, thereby inducing ferroptosis [21]. Additional evidence suggests that HSPB1 is highly expressed in glioma stem cells and contributes to ferroptosis resistance by limiting iron accumulation [22]. Consistent with these findings, we observed that HSPB1 silencing in U251 cells led to increased lipid peroxidation and Fe2+ accumulation, ultimately triggering ferroptotic cell death. Taken together, these results support the notion that HSPB1 promotes glioma cell survival, at least in part, by inhibiting ferroptosis.

Using online bioinformatics tools and literature mining, we identified BCL2-associated athanogene 3 (BAG3) as a potential HSPB1-interacting protein. This interaction was validated by coimmunoprecipitation assays. BAG3, a member of the anti-apoptotic BAG family located on chromosome 10q25, is involved in diverse cellular processes, including cell proliferation, apoptosis, cytoskeletal regulation, and protein degradation [23]. In cancer cells, which are characterized by uncontrolled growth and impaired apoptosis, BAG3 expression is frequently upregulated and contributes to tumor cell survival. In melanoma, BAG3 prevents IKK-y lysosomal degradation, thereby sustaining NF-kB activation and promoting cell survival [24]. In breast cancer, BAG3 has been implicated in cell adhesion and migration [25, 26], while deletion of its WW domain in Cos7 cells results in loss of migratory capacity. In hepatocellular carcinoma, BAG3 knockout inhibits cell



migration and invasion, and in in vivo tumor models, loss of BAG3 suppresses tumor growth and metastasis [27].

In gliomas, particularly high-grade subtypes, BAG3 is significantly overexpressed. Silencing BAG3 using siRNA has been shown to promote apoptosis in glioma cells [28]. Other studies indicate that BAG3 supports the maintenance of glioma stem-like cells and contributes to chemoresistance [29]. In line with these findings, we demonstrated that BAG3 is aberrantly overexpressed in cell lines. BAG3 knockdown significantly inhibited glioma cell proliferation and invasion, while inducing ferroptotic cell death.

Furthermore, co-transfection of BAG3 overexpression vectors into HSPB1-knockdown U251 cells partially rescued the suppressed cell growth and reversed ferroptosis induction, indicating that HSPB1 mediates its anti-ferroptotic effects through BAG3. In conclusion, both HSPB1 and BAG3 are upregulated during glioma progression. Silencing HSPB1 downregulates BAG3 expression, thereby promoting ferroptosis in glioma cells. These findings suggest that targeting the HSPB1-BAG3 axis may serve as a novel therapeutic strategy for glioma treatment.

Disclosure of conflict of interest

None.

Abbreviations

CNS, central nervous system; GPX4, glutathione peroxidase 4; ROS, reactive oxygen species; ACSL4, acyl-coA synthetase long-chain family member 4; TFR1, transferrin receptor protein 1; GSH, glutathione; HSPB1, heat shock protein family B (small) member 1; BAG3, BCL2 associated athanogene 3.

Address correspondence to: Leiming Huo, Department of Surgery II, Shenzhen Bao'an Hospital of Traditional Chinese Medicine, No. 22, 25, Yu'an 2nd Road, Bao'an District, Shenzhen 518100, Guangdong, China. E-mail: huoleiming78@gzucm.edu.cn

References

[1] Ostrom QT, Price M, Neff C, Cioffi G, Waite KA, Kruchko C and Barnholtz-Sloan JS. CBTRUS statistical report: primary brain and other cen-

- tral nervous system tumors diagnosed in the United States in 2016-2020. Neuro Oncol 2023; 25: iv1-iv99.
- [2] Wang LM, Englander ZK, Miller ML and Bruce JN. Malignant glioma. Adv Exp Med Biol 2023; 1405: 1-30.
- [3] Lei G, Zhuang L and Gan B. The roles of ferroptosis in cancer: tumor suppression, tumor microenvironment, and therapeutic interventions. Cancer Cell 2024; 42: 513-534.
- [4] Cui K, Wang K and Huang Z. Ferroptosis and the tumor microenvironment. J Exp Clin Cancer Res 2024; 43: 315.
- [5] Fu D, Wang C, Yu L and Yu R. Induction of ferroptosis by ATF3 elevation alleviates cisplatin resistance in gastric cancer by restraining Nrf2/Keap1/xCT signaling. Cell Mol Biol Lett 2021; 26: 26.
- [6] Zhang C, Zhan S, He Y, Pan Z, You Z, Zhu X and Lin Q. Inhibition of CISD2 enhances sensitivity to doxorubicin in diffuse large B-cell lymphoma by regulating ferroptosis and ferritinophagy. Front Pharmacol 2024; 15: 1482354.
- [7] Zhao Y, Liang H and Cui X. Obacunone regulates ferroptosis in ovarian cancer through the Akt/p53 pathway. Naunyn Schmiedebergs Arch Pharmacol 2025; 398: 7027-7039.
- [8] Huang W, Guo Y, Qian Y, Liu X, Li G, Wang J, Yang X, Wu M, Fan Y, Luo H, Chen Y, Zhang L, Yang N, Liu Z and Liu Y. Ferroptosis-inducing compounds synergize with docetaxel to overcome chemoresistance in docetaxel-resistant non-small cell lung cancer cells. Eur J Med Chem 2024; 276: 116670.
- [9] Chen Y, Mi Y, Zhang X, Ma Q, Song Y, Zhang L, Wang D, Xing J, Hou B, Li H, Jin H, Du W and Zou Z. Dihydroartemisinin-induced unfolded protein response feedback attenuates ferroptosis via PERK/ATF4/HSPA5 pathway in glioma cells. J Exp Clin Cancer Res 2019; 38: 402.
- [10] Chen X, Wang Z, Li C, Zhang Z, Lu S, Wang X, Liang Q, Zhu X, Pan C, Wang Q, Ji Z, Wang Y, Piao M, Chi G and Ge P. SIRT1 activated by AROS sensitizes glioma cells to ferroptosis via induction of NAD+ depletion-dependent activation of ATF3. Redox Biol 2024; 69: 103030.
- [11] Wang Z, Xia Y, Wang Y, Zhu R, Li H, Liu Y and Shen N. The E3 ligase TRIM26 suppresses ferroptosis through catalyzing K63-linked ubiquitination of GPX4 in glioma. Cell Death Dis 2023; 14: 695.
- [12] Nie XH, Qiu S, Xing Y, Xu J, Lu B, Zhao SF, Li YT and Su ZZ. Paeoniflorin regulates NEDD4L/ STAT3 pathway to induce ferroptosis in human glioma cells. J Oncol 2022; 2022: 6093216.
- [13] Li B, Zhao S, Chen Y, Gao H, Xie W, Wang H, Zhao P, Li C and Zhang Y. HSPB1 promotes tumor invasion by inducing angiogenesis in PitNETs. Endocr Relat Cancer 2024; 31: e230045.

- [14] Huo Q, Wang J and Xie N. High HSPB1 expression predicts poor clinical outcomes and correlates with breast cancer metastasis. BMC Cancer 2023; 23: 501.
- [15] Zhang G, Hu J, Li A, Zhang H, Guo Z, Li X, You Z, Wang Y and Jing Z. Ginsenoside Rg5 inhibits glioblastoma by activating ferroptosis via NR3C1/HSPB1/NCOA4. Phytomedicine 2024; 129: 155631.
- [16] Wang Z, Fang Z, Gui Y, Xi B and Xie Z. Elevated HSPB1 expression is associated with a poor prognosis in glioblastoma multiforme patients. J Neurol Surg A Cent Eur Neurosurg 2025; 86: 17-29.
- [17] An Y, Liu W, Deng Y, Huang W and Huang J. SLC7A11-HSPB1 axis: a novel mechanism for hepatocellular carcinoma progression and ferroptosis regulation. Biomed J 2025; 100869.
- [18] Meng X, Peng X, Ouyang W, Li H, Na R, Zhou W, You X, Li Y, Pu X, Zhang K, Xia J, Wang J, Zhuang G, Tang H and Peng Z. Musashi-2 deficiency triggers colorectal cancer ferroptosis by downregulating the MAPK signaling cascade to inhibit HSPB1 phosphorylation. Biol Proced Online 2023; 25: 32.
- [19] Liang Y, Wang Y, Zhang Y, Ye F, Luo D, Li Y, Jin Y, Han D, Wang Z, Chen B, Zhao W, Wang L, Chen X, Ma T, Kong X and Yang Q. HSPB1 facilitates chemoresistance through inhibiting ferroptotic cancer cell death and regulating NF-kB signaling pathway in breast cancer. Cell Death Dis 2023; 14: 434.
- [20] Chen W, Zhang X, Zhang B, Chi M and Zheng Q. HRAS induces ferroptosis through upregulating HSPB1 in hepatocellular carcinoma. Comb Chem High Throughput Screen 2024; [Epub ahead of print]
- [21] Zhang F, Wu L, Feng S, Zhao Z, Zhang K, Thakur A, Xu Z, Liang Q, Liu Y, Liu W and Yan Y. FHOD1 is upregulated in glioma cells and attenuates ferroptosis of glioma cells by targeting HSPB1 signaling. CNS Neurosci Ther 2023; 29: 3351-3363.

- [22] Wang C, Zhang M, Liu Y, Cui D, Gao L and Jiang Y. CircRNF10 triggers a positive feedback loop to facilitate progression of glioblastoma via redeploying the ferroptosis defense in GSCs. J Exp Clin Cancer Res 2023; 42: 242.
- [23] De Marco M, Turco MC and Marzullo L. BAG3 in tumor resistance to therapy. Trends Cancer 2020; 6: 985-988.
- [24] Guerriero L, Palmieri G, De Marco M, Cossu A, Remondelli P, Capunzo M, Turco MC and Rosati A. The anti-apoptotic BAG3 protein is involved in BRAF inhibitor resistance in melanoma cells. Oncotarget 2017; 8: 80393-80404.
- [25] Zhang H, Wang M, Lang Z, Liu H, Liu J and Ma L. MiR-135a-5p suppresses breast cancer cell proliferation, migration, and invasion by regulating BAG3. Clinics (Sao Paulo) 2022; 77: 100115.
- [26] Linder B, Klein C, Hoffmann ME, Bonn F, Dikic I and Kögel D. BAG3 is a negative regulator of ciliogenesis in glioblastoma and triple-negative breast cancer cells. J Cell Biochem 2022; 123: 77-90.
- [27] Lu J, Liu SY, Zhang J, Yang GM, Gao GB, Yu NN, Li YP, Li YX, Ma ZQ, Wang Y and Lu CH. Inhibition of BAG3 enhances the anticancer effect of shikonin in hepatocellular carcinoma. Am J Cancer Res 2021; 11: 3575-3593.
- [28] Antonietti P, Linder B, Hehlgans S, Mildenberger IC, Burger MC, Fulda S, Steinbach JP, Gessler F, Rödel F, Mittelbronn M and Kögel D. Interference with the HSF1/HSP70/BAG3 pathway primes glioma cells to matrix detachment and BH3 mimetic-induced apoptosis. Mol Cancer Ther 2017; 16: 156-168.
- [29] Im CN, Yun HH, Song B, Youn DY, Cui MN, Kim HS, Park GS and Lee JH. BIS-mediated STAT3 stabilization regulates glioblastoma stem celllike phenotypes. Oncotarget 2016; 7: 35056-70.